

Major Mergers and the Origin of Elliptical Galaxies

Andreas Burkert¹ and Thorsten Naab²

¹Max-Planck-Institut für Astronomie, Königstuhl 17,
D-69117 Heidelberg, Germany

²Institute of Astronomy, Madingley Road, Cambridge CB3 0HA, UK

Abstract. The formation of elliptical galaxies as a result of the merging of spiral galaxies is discussed. We analyse a large set of numerical N-Body merger simulations which show that major mergers can in principle explain the observed isophotal fine structure of ellipticals and its correlation with kinematical properties. Equal-mass mergers lead to boxy, slowly rotating systems, unequal-mass mergers produce fast rotating and disky ellipticals. However, several problems remain. Anisotropic equal mass mergers appear under certain projections disky which is not observed. The intrinsic ellipticities of remnants are often larger than observed. Finally, although unequal-mass mergers produce fast rotating ellipticals, the remnants are in general more anisotropic than expected from observations. Additional processes seem to play an important role which are not included in dissipationless mergers. They might provide interesting new information on the structure and gas content of the progenitors of early-type galaxies.

1 Introduction

Giant elliptical galaxies are believed to be very old stellar systems that formed by a major merger event preferentially very early at a high redshift of more than two (Searle et al. 1973; Toomre & Toomre 1972). The merger triggered an intensive star-formation phase which turned most of the gas of the progenitors into stars. Some fraction of the gas was heated to temperatures of order the virial temperature, producing X-ray coronae which are still visible today. The stellar disks of the progenitors were destroyed as a result of the strong tidal forces during the merger, leading to kinematically hot, spheroidal stellar remnants. Subsequently, the systems experienced very little accretion and merging with negligible star formation (Bruzual & Charlot 1993). This scenario is supported by many observations which indicate that ellipticals contain stellar populations that are compatible with purely passive evolution (Bower et al. 1992; Aragon-Salamanca et al. 1993; Ellis et al. 1997; Ziegler & Bender 1997). or with models of an exponentially, fast decreasing star formation rate (Ziegler et al. 1999).

An alternative scenario which is based on hierarchical theories of galaxy formation predicts that massive galaxies are assembled relatively late in many generations of mergers through multiple mergers of small subunits, with additional smooth accretion of gas (Kauffmann 1996; Kauffmann & Charlot 1998). In this case, ellipticals might form either if the multiple subunits are already preferentially stellar or if star formation was very efficient during the protogalactic collapse phase (Larson 1974).

The idea that ellipticals form from major mergers of massive disk galaxies has been originally proposed by Toomre & Toomre (1972). Their “merger hypothesis” has been explored in details by many authors, using numerical simulations. Gerhard (1981), Negroponte & White (1983), Barnes (1988) and Hernquist (1992) performed the first fully self-consistent merger models of two equal-mass stellar disks embedded in dark matter halos. The remnants are slowly rotating, pressure supported and anisotropic. They generally follow an $r^{1/4}$ surface density profile for radii $r \geq 0.5r_e$, where r_e is the effective radius. However it turns out that due to phase space limitations (Carlberg 1986), an additional massive central bulge component is required (Hernquist, 1993b), to fit the observed de Vaucouleurs profile (Burkert 1993) also in the inner regions. All simulations demonstrated consistently that the global properties of equal mass merger remnants resemble those of ordinary slowly rotating massive elliptical galaxies.

More recently it has become clear that ellipticals have quite a variety of fine structures with peculiar kinematical properties which, in contrast to their universal global properties, can give a more detailed insight into their formation history. It is interesting to investigate whether the merging hypothesis can explain these observations and, if yes, whether they provide more information on the validity of this scenario, the orbital parameters of the mergers and the structure and gas content of the progenitors from which the ellipticals formed.

Elliptical galaxies can be subdivided into two major groups with respect to their structural properties (Bender et al. 1988; Bender 1988a,b; Kormendy & Bender 1996). Faint ellipticals are isotropic rotators with small minor axis rotation and disky deviations of their isophotal shapes from perfect ellipses. Their isophotes are peaked in the rotational plane and a Fourier analyses of the isophotal deviation from a perfect ellipse leads to a positive value of the fourth order coefficient a_4 . These galaxies might contain secondary, faint disk components which contribute up to 30% to the total light in the galaxy, indicating disk-to-bulge ratios that overlap with those of S0-galaxies (Rix & White 1990; Scorza & Bender 1995). Disky ellipticals have power-law inner density profiles (Lauer et al. 1995; Faber et al. 1997) and show little or no radio and X-ray emission (Bender et al. 1989). Most massive ellipticals have boxy isophotes, with negative values of a_4 . They also show flat cores (Lauer et al. 1995; Faber et al. 1997) and their kinematics is more complex than that of disky ellipticals. Boxy ellipticals rotate slowly, are supported by velocity anisotropy and have a large amount of minor axis rotation. Like the secondary disks of disky ellipticals, the boxy systems occasionally reveal kinematically decoupled core components, that most likely formed from gas that dissipated its orbital energy during the merger, accumulated in the center and subsequently turned into stars (Franx & Illingworth 1988; Jędrzejewski & Schechter 1988; Bender 1988a). The cores inhibit flattened rapidly rotating disk- or torus-like stellar structures that dominate the light in the central few hundred parsecs (Rix & White 1992, Mehlert et al. 1998), but they contribute only a few percent to the total light of the galaxy. The fact that the stars are metal-enhanced confirms that gas infall and subsequently violent star formation, coupled with metal-enrichment must have played an important

role in the centers of merger remnants (Bender & Surma 1992; Davies et al. 1983; Bender et al. 1996; Davies 1996). Boxy ellipticals show strong radio emission and high X-ray luminosities, resulting from emission from hot gaseous halos (Beuing et al. 1999) that probably formed from gas heating during the merger. These hot gaseous bubbles are however absent in disk ellipticals. The distinct physical properties of disk and boxy elliptical galaxies indicate that both types of ellipticals experienced different formation histories.

In order to understand the origin of boxy and disk ellipticals the isophotal shapes of the numerical merger remnants have been investigated in detail. It has been shown that the same remnant can appear either disk or boxy when viewed from different directions (Hernquist 1993b) with a trend towards boxy isophotes (Heyl et al. 1994; Steinmetz & Buchner 1995). Barnes (1998) and Bendo & Barnes (2000) analysed a sample of disk-disk mergers with a mass ratio of 3:1 and found that the remnants are flattened and fast rotating in contrast to equal mass mergers. Naab et al. (1999) studied the photometrical and kinematical properties of a typical 1:1 and 3:1 merger remnant in details and compared the results with observational data. They found an excellent agreement and proposed that fast rotating disk elliptical galaxies can originate from purely collisionless 3:1 mergers while slowly rotating, pressure supported ellipticals form from equal mass mergers of disk galaxies.

Despite these encouraging results no systematic high-resolution survey of mergers has yet been performed to explore the parameter space of initial conditions and specify the variety of properties of merger remnants that could arise. Recently, Naab & Burkert (2003) completed a large number of 112 merger simulations of disk galaxies adopting a statistically unbiased sample of orbital initial conditions with mass ratios η of 1:1, 2:1, 3:1, and 4:1. This large sample allows a much more thorough investigation of the statistical properties of merger remnants in comparison with observed disk and boxy ellipticals.

2 The merger models

Cosmological simulations currently are not sophisticated enough to predict initial conditions of major spiral mergers. Some insight can however be gained by investigating the typical conditions under which dark matter halos merge in standard cold dark matter models. Such a detailed analysis was done by Khochfar, Burkert & White (2003). The first encounter is in most cases a parabolic orbit with an impact parameter of order the scale radius of the more massive dark halo, with random orientation of the net spin axes of the progenitors. Unequal mass mergers with mass ratios η of 3:1 to 4:1 are as likely as equal-mass mergers with $\eta = 1 : 1 - 2 : 1$. The cold dark matter simulations however do not provide information on the internal structure and gas content of the merging spirals. In fact, simulations of hierarchical structure formation including gas lead to disk galaxies which do not fit the zero point of the Tully-Fisher relation with disk scale radii that are up to a factor of 10 smaller than observed (Navarro & Steinmetz 2000). Unless these problems are solved we cannot study the subsequent

merging of disk galaxies self-consistently, including the large-scale evolution of the Universe. In the meantime, the best strategy is to construct plausible equilibrium models of disk galaxies and investigate their merging in isolation.

Equilibrium spirals were generated using the method described by Hernquist (1993a). The following units are adopted: gravitational constant $G=1$, exponential scale length of the larger disk $h = 1$ and mass of the larger disk $M_d = 1$. For a typical spiral like the Milky Way these units correspond to $M_d = 5.6 \times 10^{10} M_\odot$, $h=3.5$ kpc and a unit time of 1.3×10^7 yrs. Each galaxy consists of an exponential disk, a spherical, non-rotating bulge with mass $M_b = 1/3$ and a Hernquist density profile (Hernquist 1990) with a scale length $r_b = 0.2$. The stellar system is embedded in a spherical pseudo-isothermal halo with a mass $M_d = 5.8$, cut-off radius $r_c = 10$ and core radius $\gamma = 1$.

The mass ratios η of the progenitor disks were varied between $\eta = 1$ and $\eta = 4$. For equal-mass mergers ($\eta = 1$) in total 400000 particles were adopted with each galaxy consisting of 20000 bulge particles, 60000 disk particles, and 120000 halo particles. Twice as many halo particles than disk particles are necessary in order to reduce heating and instability effects in the disk components (Naab et al. 1999). For the mergers with $\eta = 2, 3, 4$ the parameters for the more massive galaxy were as described above. The low-mass companion however contained a fraction of $1/\eta$ less mass and number of particles in each component, with a disk scale length of $h = \sqrt{1/\eta}$, as expected from the Tully-Fisher relation (Pierce & Tully 1992).

The N-body simulations for the equal-mass mergers were performed by direct summation of the forces using the special purpose hardware GRAPE6 (Makino et al. 2003). The mergers with mass ratios $\eta = 2, 3, 4$ were followed using the newly developed treecode WINE (Wetzstein et al. 2003) in combination with the GRAPE5 (Kawai et al. 2000) hardware. WINE uses a binary tree in combination with the refined multipole acceptance criterion proposed by Warren & Salmon (1996). This criterion enables the user to control the absolute force error which is introduced by the tree construction. We chose a value of 0.001 which guarantees that the error resulting from the tree is of order the intrinsic force error of the GRAPE5 hardware which is 0.1%. For all simulations we used a gravitational softening of $\epsilon = 0.05$ and a fixed leap-frog integration time step of $\Delta t = 0.04$. For the equal-mass mergers simulated with direct summation on GRAPE6 the total energy is conserved. The treecode in combination with GRAPE5 conserves the total energy up to 0.5%.

For all mergers, the galaxies approached each other on parabolic orbits with an initial separation of $r_{sep} = 30$ length units and a pericenter distance of $r_p = 2$ length units. Free parameters are the inclinations of the two disks relative to the orbital plane and the arguments of pericenter. In selecting unbiased initial parameters for the disk inclinations we followed the procedure described by Barnes (1998). To determine the spin vector of each disk we define four different orientations pointing to every vertex of a regular tetrahedron. These parameters result in 16 initial configurations for equal mass mergers and 16 more for each mass

ratio $\eta = 2, 3, 4$ if the initial orientations are interchanged. In total we simulated 112 mergers.

In all simulations the merger remnants were allowed to settle into equilibrium approximately 8 to 10 dynamical times after the merger was complete. Then their equilibrium state was analysed.

3 Photometric and kinematical properties of the remnants

To compare our simulated merger remnants with observations we analysed the remnants with respect to observed global photometric and kinematical properties of giant elliptical galaxies, e.g. surface density profiles, isophotal deviation from perfect ellipses, velocity dispersion, and major- and minor-axis rotation. Defining characteristic values for each projected remnant we followed as closely as possible the analysis described by Bender et al. (1988a).

3.1 Isophotal shape

An artificial image of the remnant was created by binning the central 10 length units into 128×128 pixels. This picture was smoothed with a Gaussian filter of standard deviation 1.5 pixels. The isophotes and their deviations from perfect ellipses were then determined using a data reduction package kindly provided by Ralf Bender. Following the definition of Bender et al. (1988a) for the global properties of observed giant elliptical galaxies, we determined for every projection the effective a_4 -coefficient $a_{4\text{eff}}$ as the mean value of a_4 between $0.25r_e$ and $1.0r_e$, with r_e being the projected spherical half-light radius. Like for observed ellipticals we find two types of remnants. Disky systems show a positive characteristic peak of a_4 roughly at $0.5r_e$. In boxy ellipticals, the a_4 coefficient might be positive in the innermost regions. It decreases however systematically outwards with a mean value that is negative. The characteristic ellipticity ϵ_{eff} for each projection was defined as the isophotal ellipticity at $1.5r_e$. To investigate projection effects we determined for each simulation $a_{4\text{eff}}$ and ϵ_{eff} for 500 random projections of the remnant. These values were used to calculate the two-dimensional probability density function for a given simulated remnant to be "observed" in the $a_{4\text{eff}}\text{-}\epsilon_{\text{eff}}$ plane.

Figure 1 shows the ellipticities and a_4 -coefficients of mergers with $\eta = 1, 2, 3$, and 4. The contours indicate the areas of 50% (dashed line), 70% (thin line) and 90% (thick line) probability to detect a merger remnant with the given properties. Observed data points from Bender et al. (1992) are over-plotted. Filled boxes are observed boxy ellipticals with $a_{4\text{eff}} \leq 0$ while open diamonds indicate observed diskly ellipticals with $a_{4\text{eff}} > 0$. The error bar in determining a_4 from the simulations is shown in the upper left corner and was estimated applying the statistical bootstrapping method (Heyl et al. 1994). Ellipticity errors are in general too small to be visible.

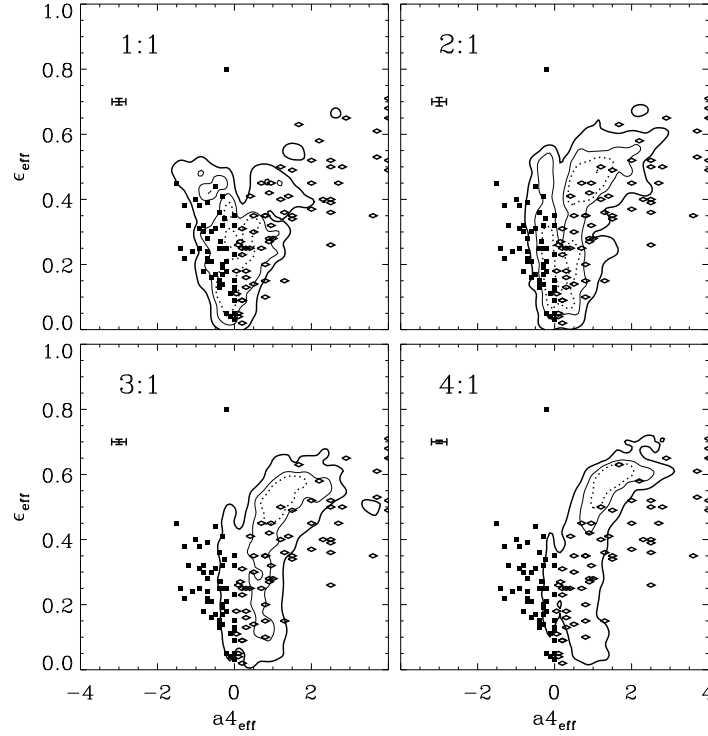


Fig. 1. Ellipticities versus fourth-order Fourier coefficient of the isophotal shape deviations is shown for simulations with different initial mass ratios. The contours indicate the 50% (dotted line), 70% (thin solid line) and the 90% (thick solid line) probability to find a merger remnant in the enclosed area. Black squares indicate values for observed boxy ellipticals, open diamonds show observed disk ellipticals.

We find that the isophotal shapes of ellipticals and their ellipticities are affected by the initial mass ratio of the merger and by projection effects. The area covered by 1:1 remnants with negative $a4_{\text{eff}}$ is in very good agreement with the observed data for boxy elliptical galaxies. In particular the observed trend for more boxy galaxies to have higher ellipticities is reproduced. However we also find configurations of 1:1 mergers which under certain projection angles appear disk with $0 \geq a4_{\text{eff}} \geq 1$. In addition, note that the remnants with $a4_{\text{eff}}$ around zero can have higher ellipticities than observed.

The distribution function of isophotal shapes for 1:1 merger remnants peaks at $a4_{\text{eff}} \approx -0.5$ (dashed curve in Fig. 2). It declines rapidly for more negative values and has a broad wing towards positive $a4_{\text{eff}}$ values. Almost half of the projected remnants are disk. In contrast, remnants of mergers with higher mass ratios shift in the direction of positive $a4_{\text{eff}}$. 2:1 remnants peak at $a4_{\text{eff}} \approx 0$. Now, 75% of the projected remnants show disk isophotes. For these cases, the observed trend of more disk ellipticals to be more flattened is also clearly

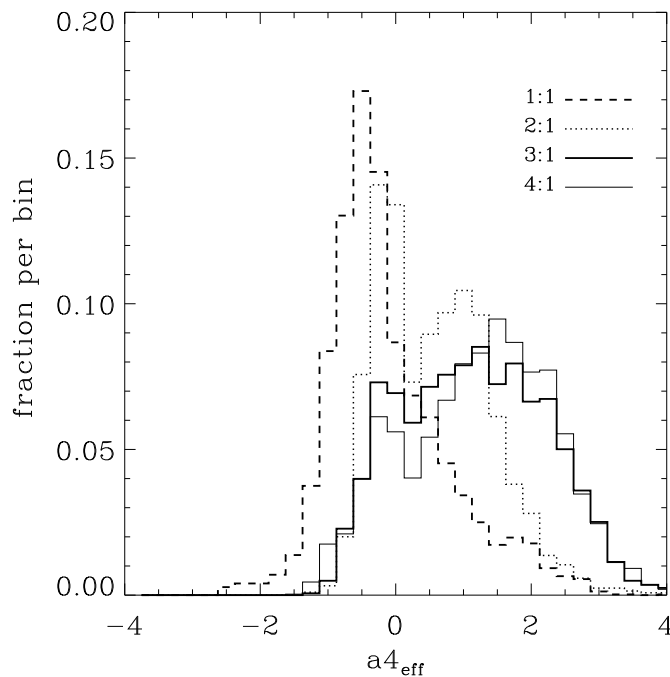


Fig. 2. Normalized histograms of the shape parameter $a4_{\text{eff}}$ for mergers with various mass ratios.

visible in Fig. 1. 3:1 and 4:1 mergers peak at $a4_{\text{eff}} \approx 1$. Their fraction of boxy projections is only 11% and 7%, respectively. The very high positive values of $a4_{\text{eff}} \geq 4$ observed in some ellipticals cannot be reproduced. One might argue that these objects formed from mergers with even higher mass ratios of $\eta \geq 5 : 1$. However, in this case, test simulations show that the merger remnants do not look like typical ellipticals anymore with characteristic de Vaucouleurs profiles as the more massive disk is not destroyed. Their surface brightness profiles instead remain exponential.

In summary, there is a clear trend for unequal-mass mergers to produce more disky remnants. Responsible for the disky appearance of the 3:1 and 4:1 remnants is the distribution of the particles of the massive disk (Barnes 1998). The particles originating from the small progenitor accumulate in a torus-like structure with peanut-shaped or boxy isophotes while the luminous material of the larger progenitor still keeps its disk-like appearance. In combination, the contribution from the larger progenitor – since it is three to four times more massive – dominates the overall appearance of the remnant. This result holds for all 3:1 and 4:1 merger remnants. For equal mass mergers however both disks are destroyed

efficiently during the merger. No dominant disk-like structure remains after the merger and the system loses the information about the initial configuration.

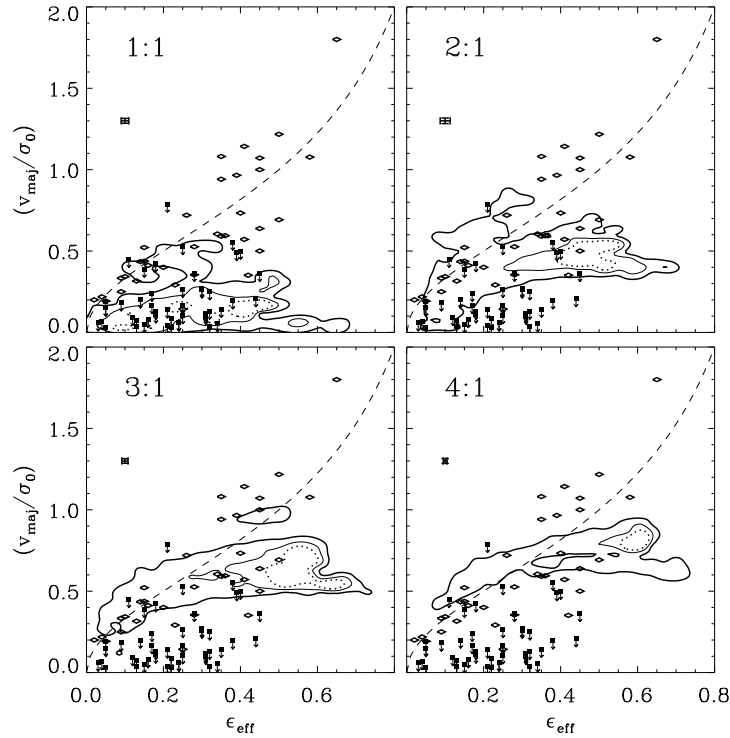


Fig. 3. Rotational velocity over velocity dispersion versus characteristic ellipticity for mergers with various mass ratios. Values for observed ellipticals are overplotted. The dashed line shows the theoretically predicted correlation for an oblate isotropic rotator.

3.2 Kinematics

The central velocity dispersion σ_0 of every remnant is determined as the average projected velocity dispersion of the stars inside a projected galactocentric radius of $0.2r_e$. The characteristic rotational velocity v_{maj} along the major axis is defined as the projected rotational velocity determined around $1.5r_e$. Like for the isophotal shape we constructed probability density plots for the kinematical properties of the simulated remnants and compared them with observational data from elliptical galaxies. Figure 3 shows the distribution function in the (v_{maj}/σ_0) - ϵ_{eff} plane.

The region of slowly rotating boxy ellipticals (filled squares) is almost completely covered by the data of 1:1 mergers. Unequal-mass merger remnants are

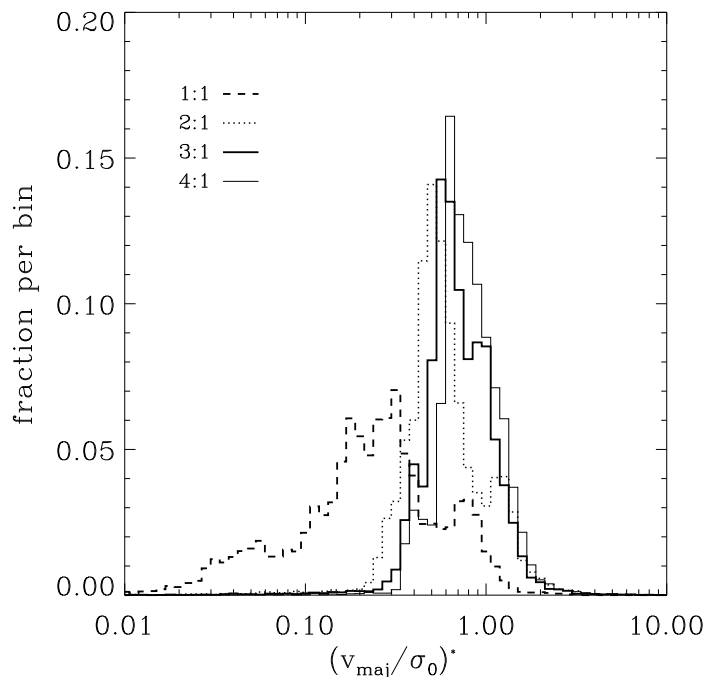


Fig. 4. Normalized histograms of $(v_{maj}/\sigma_0)^*$ for 1:1 (dashed line), 2:1 (dotted line), 3:1 (thick line) and 4:1 (thin line) mergers.

clearly fast rotating. They can be associated with disk ellipticals. Although the simulated remnants are in good agreement with observations there is again the trend for the ellipticities to be higher than observed, especially when the system is seen edge-on.

The anisotropy parameter $(v_{maj}/\sigma_0)^*$ is defined as the ratio of the observed value of (v_{maj}/σ_0) and the theoretical value for an isotropic oblate rotator $(v/\sigma)_{theo} = \sqrt{\epsilon_{obs}/(1 - \epsilon_{obs})}$ with the observed ellipticity ϵ_{obs} (Binney 1978). This parameter is frequently used by observers to test whether a given galaxy is flattened by rotation ($(v_{maj}/\sigma_0)^* \geq 0.7$) or by velocity anisotropy ($(v_{maj}/\sigma_0)^* < 0.7$) (Davies et al. 1983; Bender 1988a; Nieto et al. 1988; Scorza & Bender 1995). Figure 4 shows the normalized histograms for the $(v_{maj}/\sigma_0)^*$ values of the simulated remnants. 1:1 remnants peak around $(v_{maj}/\sigma_0)^* \approx 0.3$ with a more prominent tail towards lower values. They are consistent with being supported by anisotropic velocity dispersions. As these systems also have preferentially negative a_4 -values they agree with observations of boxy ellipticals (Fig. 5). Unequal mass mergers peak at $(v_{maj}/\sigma_0)^* \approx 0.7$, as expected for oblate isotropic rotators. Since especially the 3:1 and 4:1 remnants also have

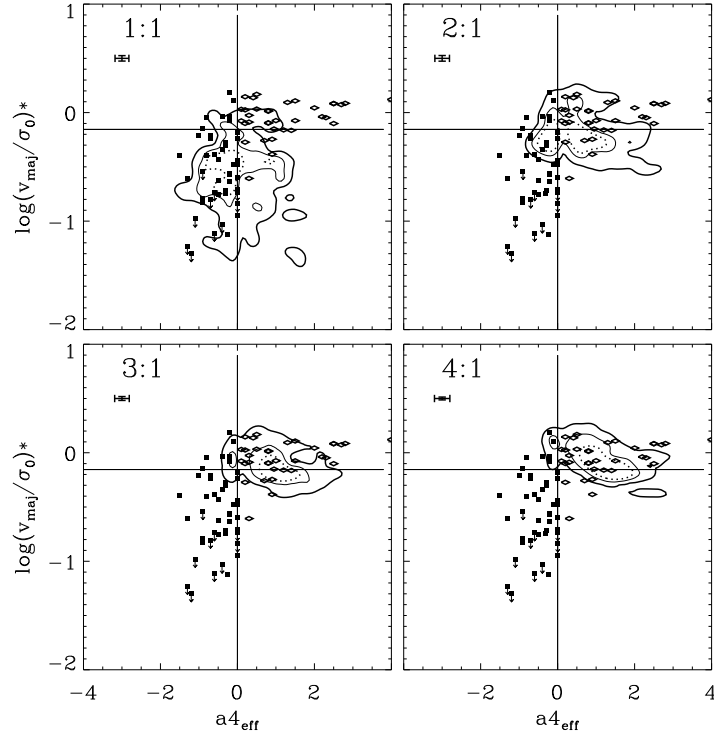


Fig. 5. Anisotropy parameter versus isophotal shape for mergers with various mass ratios. Values for observed ellipticals are overplotted.

predominantly disk isophotes they cover the area populated by observed disk ellipticals in the $\log(v_{maj}/\sigma_0)^* - a4_{eff}$ diagram which is shown in figure 5.

We also investigated the minor-axis kinematics of the simulated remnants by determining the rotation velocity along the minor axis at $0.5r_{eff}$. The amount of minor axis rotation was characterized by $(v_{min}/\sqrt{v_{maj}^2 + v_{min}^2})$ (Binney 1985). Minor axis rotation in elliptical galaxies, in addition to isophotal twist, has been suggested as a sign for a triaxial shape of the main body of elliptical galaxies (Wagner et al. 1988; Franx et al. 1991). In general, 1:1 mergers show a significant amount of minor-axis rotation, whereas 3:1 and 4:1 remnants have only small minor axis rotation (for details see Naab & Burkert 2003).

4 Conclusions

The analysis of a large set of mergers with different mass ratios and orbital geometries shows that their properties are in general in good agreement with the observational data for elliptical galaxies.

Only equal mass mergers can produce boxy, anisotropic and slowly rotating remnants with a large amount of minor axis rotation. However, in the more unlikely case that the initial spins of the progenitor disks are aligned, the remnants appear isotropic and disk-like or boxy depending on the orientation. In contrast, 3:1 and 4:1 mergers form a more homogeneous group of remnants. They have preferentially disk-like isophotes, are always fast rotating and show small minor axis rotation independent of the assumed projection. 2:1 mergers have properties intermediate between boxy or disk-like ellipticals, depending on the projection and the orbital geometry of the merger.

There still exist problems which are not solved up to now. Certain projections of 1:1 mergers lead to anisotropic, disk-like remnants which are not observed. Edge-on projections of merger remnants often show very high ellipticities $\epsilon > 0.6$ which are larger than observed. Finally, some 2:1 to 4:1 remnants are more anisotropic than expected from their rotation. Their values of $(v/\sigma)^*$ are smaller and their ellipticities are larger than observed. A problem arises especially for very low luminosity giant ellipticals which are characterized by exceptionally high rotational velocities in the outer regions that cannot be reproduced (Cretton et al. 2001). A detailed analysis of the intrinsic kinematics of disk-like, fast rotating merger unequal-mass remnants which are called isotropic due to their high $(v/\sigma)^* \approx 0.7$ demonstrates that in most cases the velocity dispersion tensor is as anisotropic as for equal-mass, boxy and anisotropic mergers with $(v/\sigma)^* = 0.1$ (Burkert et al. 2003). The anisotropy parameter therefore is not necessarily a good indicator of anisotropy. It rather measures the amount of rotation in the systems.

The present simulations were purely dissipationless, taking into account only the stellar and dark matter components. The importance of gas in determining the structure of merger remnants is not clear up to now. Kormendy & Bender (1996) proposed a revised Hubble sequence with disk-like ellipticals representing the missing link between late type systems and boxy ellipticals. They noted that gas infall into the equatorial plane with subsequent star formation could explain the origin of diskiness. Scorza & Bender (1995) demonstrated that ellipticals with embedded disks would indeed appear disk-like when seen edge-on and boxy otherwise. Although this scenario appears attractive, it cannot explain why X-ray halos are found only in boxy ellipticals. As the detection of hot gas around galaxies should be independent of their orientation, the isophotal shapes of ellipticals would not correlate with their X-ray emission, if these shapes are merely a result of projection effects.

Our simulations indicate that it is preferentially the initial mass ratio which determines the isophotal shapes of merger remnants. Still, gas could have played an important role in affecting the final structure and stellar population of ellipticals (Bekki 1998, 1999; Mihos & Hernquist 1996), not only in their central regions and might solve the problem of dissipationless mergers. Naab & Burkert (2001a) have shown that extended gas disks can form as a result of a gas rich unequal mass mergers (see also Barnes 2002). Naab & Burkert (2001b) investigated line-of-sight velocity distributions of dissipationless merger remnants and found a velocity profile asymmetry that is opposite to the observations. They

concluded that this disagreement can be solved if ellipticals would indeed contain a second disk-like substructure that most likely formed through gas accretion. The situation is however not completely clear, as another study by Bendo & Barnes (2000) found a good agreement of the observed asymmetries for some cases. More simulations, including gas and star formation will be required to understand the role of gas in mergers and to answer the question of how early-type galaxies formed.

Acknowledgement: A. Burkert thanks the organizers of the workshop "Galaxies and Chaos" for the invitation and a very stimulating conference.

References

1. Aragon-Salamanca, A. , Ellis, R. S., Couch, W. J. & Carter, D. 1993, MNRAS, 262, 764
2. Barnes, J. E. 1988, ApJ, 331, 699
3. Barnes, J. E. 1998, Galaxies: Interactions and Induced Star Formation: Lecture Notes 1996 / Saas Fee Advanced Course 26, eds. D. Friedli, L. Martinet, and D. Pfenniger, Springer, 275
4. Barnes, J. E. 2002, MNRAS, 333, 481
5. Bekki, K. 1998, ApJL, 502, L133
6. Bekki, K. 1999, ApJ, 513, 108
7. Bender, R. 1988a, A&A, 193, L7
8. Bender, R. 1988b, A&A, 202, L5
9. Bender, R., Döbereiner, S., & Möllenhoff, C. 1988, A&AS, 74, 385
10. Bender, R., Surma, P., Döbereiner, S., Möllenhoff, C. & Madejsky, R. 1989, A&A, 217, 35
11. Bender, R. & Surma, P. 1992, A&A, 258, 250
12. Bender, R. 1996, IAU Symp., 171, New Light on Galaxy Evolution, ed. R. Bender & R. L. Davies (Dordrecht: Kluwer), 181
13. Bender, R. , Burstein, D. & Faber, S.M. 1992, ApJ, 399, 462
14. Bender, R. , Ziegler, B. & Bruzual, G. 1996, ApJL, 463, L51
15. Bendo, G. J. & Barnes, J. E. 2000, MNRAS, 316, 315
16. Beuing, J., Döbereiner, S., Böhringer, H. & Bender, R. 1999, MNRAS, 302, 209
17. Binney, J. 1978, MNRAS, 183, 779
18. Binney, J. 1985, MNRAS, 212, 767
19. Burkert, A. 1993, A&A, 278, 23
20. Burkert, A., Binney, J. & Naab, T. 2003, in preparation
21. Bower, R. G., Lucey, J. R. & Ellis, R. S. 1992, MNRAS, 254, 589
22. Bruzual A., G. & Charlot, S. 1993, ApJ, 405, 538
23. Carlberg, R. G. 1986, ApJ, 310, 593
24. Cretton, N., Naab, T., Rix, H., & Burkert, A. 2001, ApJ, 554, 291
25. Davies, R. L., Efstathiou, G., Fall, S. M., Illingworth, G. & Schechter, P. L. 1983, ApJ, 266, 41
26. Davies, R. L. 1996, IAU Symp., 171, New Light on Galaxy Evolution, ed. R. Bender & R. L. Davies (Dordrecht: Kluwer), 37
27. Ellis, R. S., Smail, I. , Dressler, A. , Couch, W. J., Oemler, A. , Jr., Butcher, H. & Sharples, R. M. 1997, ApJ, 483, 582
28. Faber, S. M., et al. 1997, AJ, 114, 1771

29. Franx, M. & Illingworth, G. D. 1988, *ApJL*, 327, L55
30. Franx, M. , Illingworth, G. & de Zeeuw, T. 1991, *ApJ*, 383, 112
31. Gerhard, O.E. 1981, *MNRAS* 197, 179
32. Hernquist, L. 1990, *ApJ*, 356, 359
33. Hernquist, L. 1992, *ApJ*, 400, 460
34. Hernquist, L. 1993a, *ApJS*, 86, 389
35. Hernquist, L. 1993b, *ApJ*, 409, 548
36. Heyl, J. S., Hernquist, L. & Spergel, D. N. 1994, *ApJ*, 427, 165
37. Kawai, A., Fukushige, T., Makino, J., & Taiji, M. 2000, *PASJ*, 52, 659
38. Kauffmann, G. 1996, *MNRAS*, 281, 487
39. Kauffmann, G. & Charlot, S. 1998, *MNRAS*, 297, L23
40. Khochfar, S., Burkert, A. & White. S. 2003, in preparation
41. Kormendy, J. & Bender, R. 1996, *ApJL*, 464, L119
42. Larson, R.B. 1974, *MNRAS*, 166, 585
43. Lauer, T. R., et al. 1995, *AJ*, 110, 2622
44. Makino, J., Fukushige, T. & Namura, K. 2003, to be submitted to *PASJ*.
45. Mehlert, D., Saglia, R. P., Bender, R. & Wegner, G. 1998, *A&A*, 332, 33
46. Mihos, J. C. & Hernquist, L. 1996, *ApJ*, 464, 641
47. Naab, T. , Burkert, A., & Hernquist, L. 1999, *ApJL*, 523, L133
48. Naab, T. & Burkert, A. 2001a, *ASP Conf. Ser.* 230: *Galaxy Disks and Disk Galaxies*, 451
49. Naab, T. & Burkert, A. 2001b, *ApJL*, 555, L91
50. Naab, T. & Burkert, submitted to *ApJ*
51. Navarro, J.F. & Steinmetz, M. 2000, *ApJ*, 538, 477
52. Negroponte, J. & White, S. D. M. 1983, *MNRAS*, 205, 1009
53. Nieto, J. -L., Capaccioli, M. & Held, E. V. 1988, *A&A*, 195, L1
54. Pierce, M. J. & Tully, R. B. 1992, *ApJ*, 387, 47
55. Rix, H. -W. & White, S. D. M. 1990, *ApJ*, 362, 52
56. Rix, H. -W. & White, S. D. M. 1992, *MNRAS*, 254, 389
57. Jedrzejewski, R. & Schechter, P. L. 1988, *ApJL*, 330, L87
58. Scorza, C. & Bender, R. 1995, *A&A*, 293, 20
59. Searle, L. , Sargent, W. L. W. & Bagnuolo, W. G. 1973, *ApJ*, 179, 427
60. Steinmetz, M. & Buchner, S. 1995, *Galaxies in the Young Universe*, Proceedings of a Workshop held at Ringberg Castle, eds. H. Hippelein, K. Meisenheimer & H.-J. Röser, Springer, p. 215
61. Toomre, A. & Toomre, J. 1972, *ApJ*, 178, 623
62. Wagner, S. J., Bender, R. & Moellenhoff, C. 1988, *A&A*, 195, L5
63. Warren, M. S., & Salmon, J. K. 1996, *ApJ*, 460, 121
64. Wetzstein, M., Nelson, A., Naab, T., & Burkert, A. 2003, in preparation
65. Ziegler, B. L. & Bender, R. 1997, *MNRAS*, 291, 527
66. Ziegler, B. L., Saglia, R. P., Bender, R., Belloni, P., Greggio, L. & Seitz, S. 1999, *A&A*, 346, 13